Chemical Science

ROYAL SOCIETY OF CHEMISTRY

EDGE ARTICLE

View Article Online
View Journal | View Issue

Cite this: *Chem. Sci.*, 2024, **15**, 19770

All publication charges for this article have been paid for by the Royal Society of Chemistry

The effect of *gem*-difluorination on the conformation and properties of a model macrocyclic system†

T. J. Cogswell, ‡*[a] R. J. Lewis, [b] C. Sköld, [c] A. Nordqvist, [a] M. Ahlqvist [d] and L. Knerr *[a]

Received 13th August 2024
Accepted 1st November 2024

DOI: 10.1039/d4sc05424e

rsc.li/chemical-science

Conformational control of drug candidates to engineer improved potency and ADME properties is an ongoing area of research. Macrocyclic rings tend to offer a greater degree of rigidity than non-cyclised small molecules, and, as a result they are perfect platforms to instil conformational controls. In this study, the difluoroalkoxyphenyl moiety is examined as a tool to alter the conformation of macrocycles. A fluorinated and non-fluorinated macrocyclic matched pair is compared in terms of conformation preferences and related ADME properties. The synthesised macrocycles are found to give similar major conformations exhibiting a *trans* amide in the macrocyclic backbone. However, for the fluorinated macrocycle, the major *trans* amide conformation is in equilibrium with a *cis* amide minor conformation, seen by ^{1}H NMR in a 4 : 1 ratio of *trans*/*cis*. The conformational fits for the minor fluorinated isomer demonstrate the out of plane preference of the difluoroalkoxy system encouraging the amide within the macrocycle backbone to adopt a *cis* conformation. The fluorinated macrocycle was less metabolically stable compared to the non-fluorinated, postulated to be a result of the interconversion of *trans* amide to the *cis* amide, which potentially could be more readily metabolised.

Introduction

In the past decade, there has been an intense renewed interest in 'beyond the rule of five' modalities in drug discovery.[1] As the complexity and diversity of protein targets and drug mechanisms of action increase, medicinal chemists need to access a broader range of modalities.[2] Macrocycles can offer unique advantages over traditional small molecules with the cyclic structure conveying an innate preorganization on the molecular conformation.[3] This cyclic nature results in a lowered entropic penalty on target binding, that can lead to higher target affinity and selectivity, especially important when targeting extended binding pockets and macromolecular interactions.[4] Nature has made full use of this phenomenon, with 20% of all known natural products being macrocyclic.[5] However, even with the numerous reports documenting the benefits of macrocyclization on the potency of drug candidates,[6] a lack of understanding on how to best modulate their physicochemical properties and cell permeabilities to produce robust clinical candidates remains.[7] As a result, macrocycles remain an underexploited modality in drug discovery.[3]

To capitalize on the preorganisation of macrocyclic structures, there is a significant interest into ways to bias and alter the conformation of macrocycles to optimize their target binding interactions through a rational design approach.[8] Common approaches include the incorporation of stereocenters,[9] the addition of alkyl groups to backbone atoms,[10] and the installation of both saturated and unsaturated heterocycles into the macrocyclic backbone.[11] One interesting approach takes advantage of the stereoelectronic interactions that polarized C–F bonds have on neighbouring groups, where orbital alignments favour stabilized conformations.[12] Incorporation of fluorine atoms has previously been identified as a means to change conformational preference in many functional systems such as organocatalysis,[13] pharmaceuticals,[14] and liquid crystals.[15]

In a seminal publication in 2014, Hunter *et al.* reported the use of the fluorine gauche effect to demonstrate, for the first time, that stereoselective fluorination could alter the conformation of a peptidic macrocycle.[16] Each synthesised isomer of the vicinal fluorinated Unguisin A occupied a unique low energy

[a]*Medicinal Chemistry, Early Cardiovascular, Renal and Metabolism, BioPharmaceuticals R&D, AstraZeneca, Gothenburg, Sweden. E-mail: thomas.cogswell@acerta-pharma.com; laurent.knerr@astrazeneca.com*

[b]*Medicinal Chemistry, Early Respiratory and Immunology, BioPharmaceuticals R&D, AstraZeneca, Gothenburg, Sweden*

[c]*Drug Design and Discovery, Department of Medicinal Chemistry, BMC, Uppsala University, P.O. Box 574, SE751 23 Uppsala, Sweden*

[d]*DMPK, Early Cardiovascular, Renal and Metabolism, BioPharmaceuticals R&D, AstraZeneca, Gothenburg, Sweden*

† Electronic supplementary information (ESI) available. See DOI: https://doi.org/10.1039/d4sc05424e

‡ Current address: Acerta Pharma B.V., A Member of the AstraZeneca Group, Kloosterstraat 9, 5349 AB, Oss, The Netherlands.

conformation which differed from the parent non-fluorinated compound. In 2016, O'Hagan and co-workers found that when installing a CF_2-group into different positions of the aliphatic backbone of a family of musk lactones, the macrocyclic ring was constrained into a rectangular conformation with the CF_2-group always situated at a corner site.[17]

In a non-macrocyclic system, Durley and co-workers reported an intriguing fluorination effect whilst developing a library of cholesteryl ester transfer protein (CETP) inhibitors.[18] When compared to the alkoxyphenyl analogue **1**, the incorporation of a fluorinated side chain in **2** led to an 8-fold increase in potency which was attributed to a more optimal configuration adopted within the enzyme active site (Fig. 1A). After studying the conformation through *ab initio* calculations, they confirmed that the non-fluorinated alkyl chain of **1** aligned with the plane of the aromatic ring whereas the fluorinated chain occupied an orthogonal conformation.[19] This rotation of the OCF_2 bond allowed the lone pairs of the oxygen to donate into the low lying σ^*_{CF} antibonding orbitals leading to a stabilization of the orthogonal conformation (Fig. 1B). Since this first example, O'Hagan reported that the same conformational effect also occurs when a sulfur linker replaces the oxygen.[20]

A survey of available crystallographic data for difluoromethoxyaryl-containing structures supported by density functional theory (DFT) calculations confirmed that the orthogonal arrangement of two *endo* fluorines was one of the two major conformations adopted by this module.[21] An *endo–exo* arrangement was also predicted to have a similar energy in the gas phase leading to postulations that, due to this low barrier to rotation, this module has the potential to access different conformations when subjected to different micro-environments.[22]

Intrigued by the reported impact of the *gem*-difluorination of alkoxyphenyl group in acyclic systems, we decided to expand these studies by incorporating this fluorinated module into a macrocyclic core. While there is some exemplification of this chemistry in recent patent literature,[23] there is still very little data reported on the impact of that design on the macrocycle properties. Therefore, we aimed to expand the toolbox of small, fluorinated units available to increase the conformational diversity and adaptability of macrocyclic scaffolds. Conformational changes through fluorination has been shown to alter physicochemical properties such as polarity, permeability, and solubility, therefore, an in-depth study into these relationships was also conducted.[24]

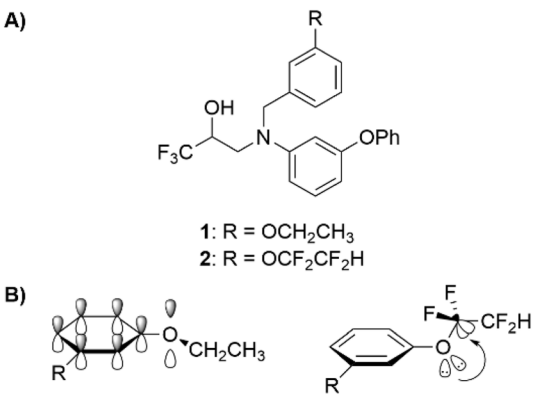

Fig. 1 (A) The structures of CETP inhibitors reported by Durley and co-workers.[19] The non-fluorinated analogue **1** has a IC_{50} of 1.6 μM while the fluorinated analogue **2** has an IC_{50} of 0.2 μM. The values were determined in a buffer transfer assay. (B) Hyperconjugative π–σ* C–F interaction rationale for the reduced in-plane conformational preference of a fluoroalkoxyaryl group.[19]

Results and discussion

Synthesis

To study this fluorination effect in macrocycles a model system was selected, based on the BACE-1 inhibitor **3**. This was envisaged to provide entry into a simplified and medicinal chemistry relevant macrocycle ring system (Fig. 2).[25]

The fluorinated and non-fluorinated macrocycles **4a** and **4b** were prepared using the synthetic route reported in Scheme 1. The 1,1-difluorinated allylated phenol starting material **5a** was synthesised in a previous publication from our laboratories utilizing methodology developed by Ichikawa *et al.*[26,27] The starting materials (**5a** and **6**) were combined through a Heck reaction followed by hydrogenation providing **8a** in good yield. Ester hydrolysis and Boc deprotection gave the precyclisation precursor, that upon macrolactamisation yielded the desired macrocyclic scaffold **4a**. Using the same synthetic route, the non-fluorinated match pair macrocycle **4b** was also prepared.

For macrocycle **4a**, two unexpected features of the proton NMR spectrum were immediately apparent (Fig. 3). Firstly, two conformations were visible in an approximate ratio of 4 : 1 with slow exchange on the NMR timescale. Secondly, the minor

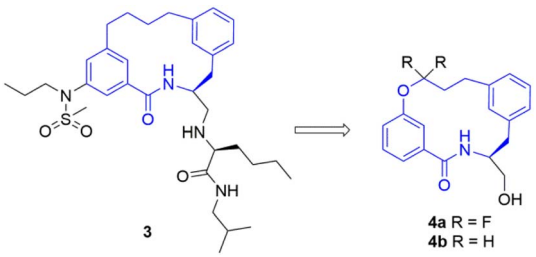

Fig. 2 The structure of a BACE-1 inhibitor **3** developed by researchers at Merck for the treatment of Alzheimer's disease (left).[25] The target model macrocyclic structures **4a** and **4b** to be studied herein (right).

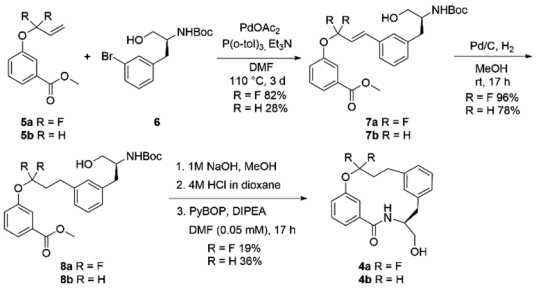

Scheme 1 The synthesis of the model fluorinated macrocycle and non-fluorinated match pair.

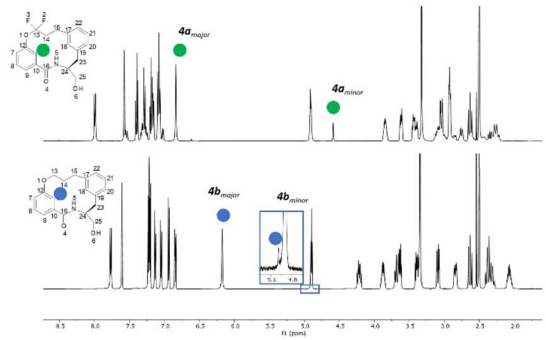

Fig. 3 The stacked ^{1}H NMR spectra in DMSO-d_6 of the non-fluorinated macrocycle **4b** (top) and fluorinated macrocycle **4a** (bottom).

conformation exhibited a highly shielded aromatic proton at 4.59 ppm. This signal was 2.2 ppm more shielded than the equivalent proton in the major conformation. Most other protons exhibited differences in chemical shift of 0.2 to 0.9 ppm between the conformations. This conformational signature suggests a significant change in conformation between major and minor forms.

In contrast, the proton spectrum for non-fluorinated macrocycle **4b** did not clearly exhibit slowly exchanging conformations, though a ROESY NMR experiment did reveal the presence of a second conformation (visible as exchange cross peaks from certain protons – see ESI†). The ratio between the major and minor forms was 200 : 1, a significant difference to that observed in **4a**.

Conformational analysis

To investigate the influence of the difluoromethoxyaryl system on the conformation of the macrocyclic backbone of **4a** and **4b**, calculated conformations were fit to experimental NMR data using the Mspin program.[28] The results of the MSpin program was confirmed by an independent fit of the major conformations using a least squares approach using QM optimized conformations.

Conformational searches for both **4a** and **4b** were performed that contained examples of both *cis* and *trans* amides. After QM optimization, data was fit in the MSpin program using proton–proton NOE distances, coupling constants and calculated proton chemical shifts. The use of chemical shifts was especially important for the minor conformation as only a few proton–proton NOE distances could be accurately determined. Proton-fluorine NOEs were used qualitatively to distinguish between the different conformational fits found for **4a**.

For the major conformation of **4a** (**4a$_{major}$**), two conformations were found, approximately equally distributed, accounting for about 90% of the population (Fig. 4). The two conformations differ from each other primarily in the relative orientations of the two aromatic rings.

For the minor conformation of **4a** (**4a$_{minor}$**), the same procedure was followed to yield a fit composed of two conformers **4a$_{minor}$_#1** at 65% and **4a$_{major}$_#2** at 30% (Fig. 5). Interestingly, the conformers both bear the *cis* amide in place of the *trans*, demonstrating a significantly different conformation compared to **4a$_{major}$**. The highly shielded proton seen in the NMR spectrum (Fig. 3), was found to make an edge/face interaction with the second aromatic ring accounting for the unusual shielding.[29]

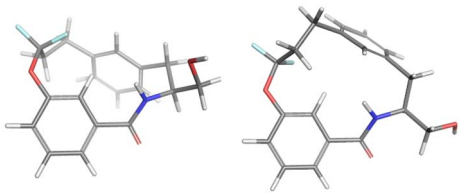

Fig. 4 Conformations **4a$_{major}$_#1** and **4a$_{major}$_#2** from Mspin making up 90% of the population of **4a$_{major}$**.

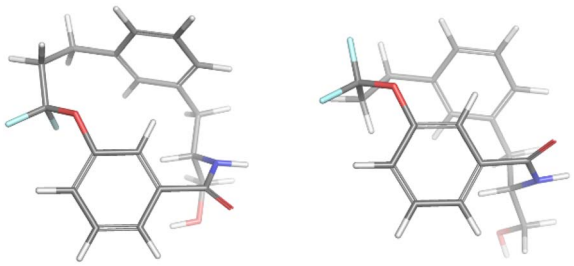

Fig. 5 The conformational fits from Mspin for **4a$_{minor}$**. Two *cis* amides **4a$_{minor}$_#1** (left) and **4a$_{minor}$_#2** at 30% (right).

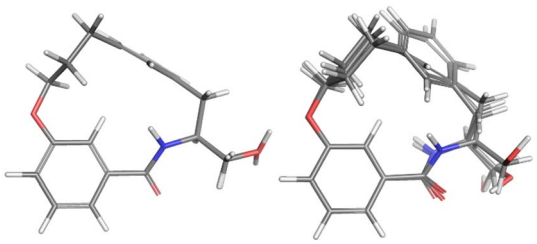

Fig. 6 The conformational fits from Mspin for **4b**. The overlay consisting of conformations **4b_#1** and **4b_#2** (left). The overlay of conformations **4b_#3**, **4b_#4** and **4b_#5** accounting for 25% of the population (right).

A similar approach was followed to find two clusters of similar conformations for the non-fluorinated macrocycle **4b**. The two clusters are shown in Fig. 6. On the left are two conformations differing only in the OH bond orientation accounting for 55% of the population and on the right, three conformations accounting for 25% of the population which differ in OH orientation and the amide bond portion of the macrocycle.

The results from Mspin were compared with conformations selected by comparing the sum of the absolute difference between the experimentally derived ^{1}H–^{1}H NOE distances for **4a** and **4b** respectively (See ESI†) and the corresponding atom distance of a calculated conformational ensemble after QM optimization.

Table 1 *In vitro* and physicochemical profiling of macrocycles **4a** and **4b**

	Fluorinated macrocycle **4a**	Non-fluorinated macrocycle **4b**
log $D_{7.4}$	2.4	2.4
ePSA (Å^2)	70	69
Human hepatocytes metabolic stability $t_{1/2}$ (min)	<2.3	10
Human liver microsomes metabolic stability $t_{1/2}$ (min)	<2.3	31
Chemical stability Aq. pH1 $t_{1/2}$ (h)	11	>72
Chemical stability Aq. pH7.4 $t_{1/2}$ (h)	>72	>72
Chemical stability Aq. pH10 $t_{1/2}$ (h)	>72	>72
Solubility (μM)	21	243
Intrinsic permeability Caco AB pH 6.5 (inhibition) P_{app} (1×10^{-6} cm s^{-1})	96	74

A combination of two conformations was proposed for **4a$_{major}$** since both fluorine substituents displayed a strong ^{1}H–^{19}F NOE to H11. These two conformations agreed with the solutions found by Mspin (Fig. 4). For **4b** an overall best fit was found for a conformation comprising a *trans* amide bond and the ether substituent in the plane of the phenyl ring, this also best reflected one of the suggested solutions from Mspin (Fig. 6).

The fluorinated analogue **4a** is expected to prefer that the O–CF_2 bond is out of plane of the bonded aromatic ring. However, this bond is constrained by being part of a macrocyclic ring, thus moving this bond out of plane likely introduces higher energy conformational elements elsewhere in the macrocycle. These conformational compromises can be seen born out in conformations **4a$_{major}$_#1**, **4a$_{major}$_#2**, **4a$_{minor}$_#1** and **4a$_{minor}$_#2**. Conformation **4a$_{major}$_#2** is similar to the **4b** conformations in that the O–CF_2 bond is almost co-planar with the aromatic ring and the ideal chain geometry is only slightly distorted (maximum deviation 18°). In conformation **4a$_{major}$_#1** however, the O–CF_2 bond is 32° out of plane from the aromatic ring but the ideal chain geometry is more distorted (maximum deviation 37°). When the amide is in a *cis* geometry (conformations **4a$_{minor}$_#1** and **4a$_{minor}$_#2**), the O–CF_2 bond can move further out of plane (60° and 46°) and the ideal chain geometry is less distorted (maximum deviation 23°). This comes at the expense of some greater deviation from planarity of the amide bond (36° and 27°). **4b** adopts a conventional conformation with a *trans* amide bond and has torsion angles of bonded sp^3 atoms (*syn*, *anti*, *gauche*) deviating by no more than 12° from an ideal chain (+60°, 180°, −60°). The macrocyclic O–CH_2 bond is within 6° of co-planarity of the aromatic ring except in conformation **4b_#5** when it is 15° out of plane. The amide bond is distorted from planarity by 12–17°. Full details of the torsions observed can be seen in Table S3.†

Using the ratios of *trans* to *cis* conformer for **4a** and **4b**, it is possible to estimate an energy penalty of at least 10 kJ mol^{-1} for positioning the fluorine atoms approximately in plane with the aromatic ring compared to the proton atoms. This assumes only that the remote fluorine proton exchange has no direct effect on the energetics of the amide bond.

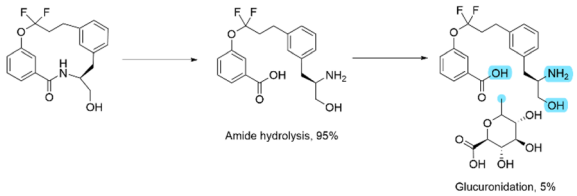

Scheme 2 The metabolism profile of **4a** upon incubation with human hepatocytes. The percentage values are semi-quantitative, based on MS-response. Where the exact position of glucuronidation could not be determined, the potential sites are labelled in blue.

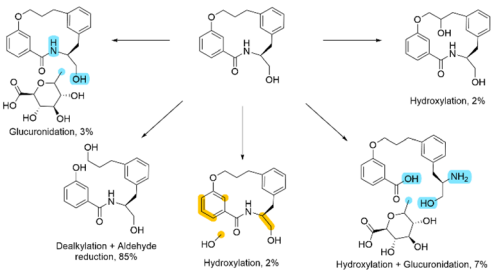

Scheme 3 The metabolism profile of **4b** upon incubation with human hepatocytes. The percentage values are semi-quantitative, based on MS-signal. Where the exact positions could not be determined, the potential sites of glucuronidation are labelled in blue and the potential sites of oxidation labelled in orange.

Physicochemical and ADME properties

To explore further the effects of fluorination on the macrocycle, *in vitro* physicochemical and ADME profiling was performed, and the two systems compared head-to-head (Table 1). The fluorination effect on measured lipophilicity (log $D_{7.4}$) was minimal, which is consistent with literature reports.[3] The intrinsic permeability between the two macrocycles was also comparable, with **4a** and **4b**, having P_{app} values of 96 and 74, respectively, in the Caco-2 *in vitro* assay. Interestingly, a 10-fold difference in solubility between the two systems was identified, which was not correlated with any significant measured lipophilicity or polarity (as measured by ePSA)[30] differences.

A difference in the metabolic stability was observed between the two systems. In both human hepatocytes and human liver microsomes, the half-life ($t_{1/2}$) of fluorinated **4a** was below a measurable time point whereas the non-fluorinated **4b** had a $t_{1/2}$ of 10 and 31 minutes respectively.

At first glance, this result seems to be counter intuitive as fluorination has been widely reported to improve the metabolic stability of drug candidates.[31] To look in more detail, a metabolic stability study was undertaken to identify the metabolites in both the fluorinated and non-fluorinated examples upon incubation in human hepatocytes (Schemes 2 and 3). The amide of **4a** was found to be rapidly hydrolysed to the open compound

as a major metabolite. Whereas **4b** showed little amide hydrolysis and instead was predominantly dealkylated at the phenolic site leading to the phenol derivative as the main metabolite. As expected, the fluorinated macrocycle was completely protected from this dealkylation metabolic pathway. We postulate that the presence of a significant *cis* amide population due to the conformational impact of the *gem*-difluorinated system is a major driver in the promotion of metabolism through amide cleavage. This represented a dramatic switch of metabolism pathway upon fluorination and whilst the magnitude is surprising in this case similar effect has been previously reported in the literature.[32]

To understand the chemical stability profiles of both macrocycles, we complemented the metabolization study with hydrolytic stability studies at pH 1, 7.4 and 10. We could show that, except for the lesser stability of fluorinated macrocycle in acidic conditions (half-life 11 hours at pH 1), both scaffolds were similarly stable with half-lives above 3 days in all conditions tested. Based on pK_a measurements for two benzoic acids possessing the fluorinated and non-fluorinated allyloxy groups (see ESI†) we could also verify that the inductive electron withdrawing effect of the fluorinated analogue was modest thus strengthening the evidence for impact on chemical stability of this fluorinated module being limited.

Additionally, we could show that the fluorinated analogue peculiar metabolic stability profile was specific to the macrocyclic scaffold by studying a matched pair of related linear analogues (see ESI†). Interestingly this demonstrated that while the linear non-fluorinated analogue showed comparable stability to its macrocyclic counterpart, the stability of the linear fluorinated analogue was considerably higher than the fluorinated macrocycle based on their half-lives upon incubation with human microsomes or human hepatocytes. The improved stability for the linear fluorinated analogue could not be attributed to a change in lipophilicity as both fluorinated analogues had a log $D_{7.4}$ of 2.4.

Conclusions

To study the conformational effects that *gem*-difluorination has on a macrocyclic system, model fluorinated and non-fluorinated match pair **4a** and **4b** were synthesized. The measured NMR data of **4a** and **4b** were input into MSpin software to identify likely conformational fits. The fluorinated macrocycle was found to have two conformations on the NMR timescale in a ratio of 4 : 1 whereas the non-fluorinated analogue favours a single conformation with a 200 : 1 ratio. The conformational fits for $\mathbf{4a_{major}}$ and **4b** showed the alkoxy phenyl chain to be in a similar geometry and a *trans* amide present on the other side of the macrocyclic scaffold. However, the fit for $\mathbf{4a_{minor}}$ showed an altered geometry of the fluorinated chain and, seemingly to allow this to occur within the macrocycle, an edge/face interaction between the two aromatic rings and the *cis* amide were present. Using the difference in ratio between the *cis* : *trans* conformers of **4a** and **4b**, we were able to estimate the strength of the fluorination effect to be at least 10 kJ mol^{-1}.

The physicochemical and ADME properties for **4a** and **4b** were examined, revealing a difference in metabolic stability in both human hepatocytes and human liver microsomes between the two macrocycles. Metabolite identification studies revealed that for **4a**, amide cleavage was the predominant metabolic pathway, whereas this was a minor pathway for **4b**.

This is the first time this *gem*-difluorinated alkoxyphenyl conformational effect has been demonstrated experimentally in a macrocyclic system and, interestingly, it was found to have a profound effect on the properties of the compound. The fluorination pattern studied here represents another potential conformational design tool to modulate the conformer population of macrocyclic scaffolds and optimize their interaction with biological targets. Future work to install this group into a diverse array of macrocyclic rings could shed further light on how this effect could be harnessed to tune the conformations of macrocycles. The inclusion of this motif into an active medicinal chemistry regime where target-binding and target-selectivity data are generated represents an important future goal for this area of research.

Data availability

The data supporting this article have been included as part of the ESI.†

Author contributions

TC: conceptualization, data curation, formal analysis, investigation, methodology, validation, visualization, writing – original draft, writing – review & editing. RJL: conceptualization, data curation, formal analysis, investigation, methodology, writing – original draft, writing – review & editing. CS: conceptualization, writing – review & editing. AN: molecular modelling calculations and fitting conformations to calculated NOE distances, writing – review & editing. MA: data curation, investigation, visualization, writing – review & editing. LK: conceptualization, investigation, project administration, supervision, writing – original draft, writing – review & editing.

Conflicts of interest

RJL, AN, MA and LK are employed by AstraZeneca and RJL, AN, MA and LK own shares in the company. TC is currently employed by Acerta Pharma, a member of the AstraZeneca group. The postdoctoral position of TC, at the time the work was undertaken, was part funded by AstraZeneca.

Acknowledgements

This work was supported by the Initial Training Network, FLUOR21(TC), funded by the FP7 Marie Curie Actions of the European Commission (FP7-PEOPLE-2013-ITN-607787). The authors would like to acknowledge the support of the ADME group of AstraZeneca Gothenburg. CS acknowledges support from KLOSS Akademi Ut (INNOV 2015/29) and Vinnova (grant no. 2016-02110).

Notes and references

1 (*a*) M.-Q. Zhang and B. Wilkinson, *Curr. Opin. Biotechnol.*, 2007, **18**(6), 478–488; (*b*) B. C. Doak, B. Over, F. Giordanetto and J. Kihlberg, *Chem. Biol.*, 2014, **21**(9), 1115–1142; (*c*) G. B. Santos, A. Ganesn and F. S. Emery, *ChemMedChem*, 2016, 2245–2251; (*d*) D. A. DeGoey, H.-J. Chen, P. B. Cox and M. D. Wendt, *J. Med. Chem.*, 2018, **61**(7), 2636–2651.

2 (*a*) S. Surade and T. L. Blundell, *Chem. Biol.*, 2012, **19**(1), 42–50; (*b*) E. Valeur, S. M. Guéret, H. Adihou, R. Gopalakrishnan, M. Lemurell, H. Waldmann, T. N. Grossmann and A. T. Plowright, *Angew. Chem., Int. Ed.*, 2017, **56**(35), 10294–10323.

3 (*a*) E. M. Driggers, S. P. Hale, J. Lee and N. K. Terrett, *Nat. Rev. Drug Discov.*, 2008, **7**, 608–624; (*b*) V. Marti-Centelles, M. D. Pandey, M. I. Burguete and S. V. Luis, *Chem. Rev.*, 2015, **115**, 8736–8834; (*c*) A. K. Yudin, *Chem. Sci.*, 2015, **6**, 30–49.

4 (*a*) J. Mallinson and I. Collins, *Future Med. Chem.*, 2012, **4**(11), 1409–1438; (*b*) A. Russo, C. Aiello, P. Grieco and D. Marasco, *Curr. Med. Chem.*, 2016, **23**(8), 748–762.

5 A. T. Frank, S. N. Farina, N. Sawwan, O. R. Wauchope, M. Qi, E. M. Brzostowska, W. Chan, F. W. Grasso, P. Haberfield and A. Greer, *Mol. Diversity*, 2007, **11**, 115–118.

6 For selected examples see: (*a*) N. Proisy, S. Y. Sharp, K. Boxall, S. Connelly, S. M. Roe, C. Prodromou, A. M. Z. Slawin, L. H. Pearl, P. Workman and C. J. Moody, *Chem. Biol.*, 2006, **13**(11), 1203–1215; (*b*) Z.-F. Tao, L. Wang, K. D. Stewart, Z. Chen, W. Gu, M.-H. Bui, P. Merta, H. Zhang, P. Kovar, E. Johnson, C. Park, R. Judge, S. Rosenburg, T. Sowin and N.-H. Lin, *J. Med. Chem.*, 2007, **50**(7), 1514–1527; (*c*) U. Lücking, G. Siemeister, M. Schäfer, H. Briem, M. Krüger, P. Lienau and R. Jautelat, *ChemMedChem*, 2007, **2**(1), 63–77; (*d*) J. E. DeLorbe, J. H. Clements, B. B. Whiddon and S. F. Martin, *ACS Med. Chem. Lett.*, 2010, **1**(8), 448–452; (*e*) D. I. Oumana, N. K. Yilmaz, K. L. Prachanronarong, C. A. A. Ali and C. A. Schiffer, *ACS Chem. Biol.*, 2016, **11**(4), 900–909.

7 (*a*) F. Giordanetto and J. Kihlberg, *J. Med. Chem.*, 2014, **57**(2), 278–295; (*b*) D. S. Nielson, H. N. Hoang, R.-J. Lohman, T. A. Hill, A. J. Lucke, D. J. Craik, D. J. Edmonds, D. A. Griffith, C. J. Rotter, R. B. Ruggeri, D. A. Price, S. Liras and D. P. Fairlie, *Angew. Chem., Int. Ed.*, 2014, **53**, 12059–12063; (*c*) A. T. Bockus, K. W. Lexa, C. R. Pye, A. S. Kalgutkar, J. W. Gardner, K. C. R. Hund, W. H. Hewtt, J. A. Schwochert, E. Glassey, D. A. Price, A. M. Mathiowetz, S. Liras, M. P. Jacobson and R. S. Lokey, *J. Med. Chem.*, 2015, **58**(11), 4581–4589; (*d*) B. Over, P. Matsson, C. Tyrchan, P. Artursson, B. C. Doak, M. A. Foley, C. Hilgendorf, S. E. Johnston, M. D. Lee IV, R. J. Lewis, P. McCarren, G. Muncipinto, U. Norinder, M. W. D. Perry, J. R. Duvall and J. Kihlberg, *Nat. Chem. Biol.*, 2016, **12**, 1065–1074.

8 (*a*) D. P. Fairlie, G. Abbenante and D. R. March, *Curr. Med. Chem.*, 1995, **2**, 654–686; (*b*) J. E. Bock, J. Gavenonis and J. A. Kritzer, *ACS Chem. Biol.*, 2013, **8**, 488–499; (*c*) M. Porel, D. N. Thornlow, N. N. Phan and C. A. Alabi, *Nat. Chem.*, 2016, **8**, 590–596; (*d*) S. D. Appavoo, S. Huh, D. B. Diaz and A. K. Yudin, *Chem. Rev.*, 2019, **119**, 9724–9752.

9 For selected examples see: (*a*) M. P. Glenn, M. J. Kelso, J. D. A. Tyndall and D. P. Fairlie, *J. Am. Chem. Soc.*, 2003, **125**, 640–641; (*b*) A. Sharma, S. Sharma, R. P. Tripathi and R. S. Ampapathi, *J. Org. Chem.*, 2012, **77**, 2001–2007.

10 For selected examples see: (*a*) H. Luesch, W. Y. Yoshida, R. E. Moore and V. J. Paul, *Bioorg. Med. Chem.*, 2002, **10**, 1973–1978; (*b*) T. W. Johnson, P. F. Richardson, S. Bailey, A. Brooun, B. J. Burke, M. R. Coillins, J. J. Cui, J. G. Deal, Y.-L. Deng, D. Dihn, *et al.*, *J. Med. Chem.*, 2014, **57**, 4720–4744; (*c*) J. Elleraas, J. Ewanicki, T. W. Johnson, N. W. Sach, M. R. Collins and P. F. Richardson, *Angew. Chem.*, 2016, **128**, 3654–3659.

11 For selected examples see: (*a*) S. Zaretsky, C. G. Scully, A. J. Lough and A. K. Yudin, *Chem.–Eur. J.*, 2013, **19**, 17668–17672; (*b*) J. R. Frost, C. G. Scully and A. K. Yudin, *Nat. Chem.*, 2016, **8**, 1105–1111.

12 (*a*) B. E. Smart, *J. Fluorine Chem.*, 2001, **109**, 3–11; (*b*) D. O'Hagan, *Chem. Soc. Rev.*, 2008, **37**, 308–319; (*c*) L. Hunter, *Beilstein J. Org. Chem.*, 2010, 38, DOI: **10.3762/bjoc.6.38**.

13 L. E. Zimmer, C. Sparr and R. Gilmour, *Angew. Chem., Int. Ed.*, 2011, **50**, 11860–11871.

14 N. A. Meanwell, *J. Med. Chem.*, 2018, **61**(14), 5822–5880.

15 M. Hird, *Chem. Soc. Rev.*, 2007, **36**, 2070–2095.

16 X.-G. Hu, D. S. Thomas, R. Griffith and L. Hunter, *Angew. Chem., Int. Ed.*, 2014, **53**, 6176–6179.

17 (*a*) M. J. Corr, R. A. Cormanich, C. N. von Hahmann, M. Bühl, D. B. Cordes, A. M. Z. Slawin and D. O'Hagan, *Org. Biomol. Chem.*, 2016, **14**, 211–219; (*b*) R. Callejo, M. J. Corr, M. Yang, D. B. Cordes, A. M. Z. Slawin and D. O'Hagan, *Chem.–Eur. J.*, 2016, **22**(24), 8137–8151.

18 R. C. Durley, M. L. Grapperhaus, M. A. Massa, D. A. Mischke, B. L. Parnas, Y. M. Fobian, N. P. Rath, D. D. Honda, M. Zeng, D. T. Connolly, D. M. Heuvelman, B. J. Witherbee, K. C. Glenn, E. S. Krul, M. E. Smith and J. A. Sikorski, *J. Med. Chem.*, 2000, **43**(24), 4575–4578.

19 M. A. Massa, D. P. Spangler, R. C. Durley, B. S. Hickory, D. T. Connolly, B. J. Witherbee, M. E. Smith and J. A. Sikorski, *Bioorg. Med. Chem. Lett.*, 2001, **11**, 1625–1628.

20 R. Tomita, N. Al-Maharik, A. R. Garcia, M. Bühl and D. O'Hagan, *Org. Biomol. Chem.*, 2018, **16**, 1113–1117.

21 (*a*) *CSD Version 5.37*; (*b*) K. Müller, C. Faeh and F. Diederich, *Science*, 2007, **317**, 1881–1886.

22 Q. A. Huchet, N. Trapp, B. Kuhn, B. Wagner, H. Fischer, N. A. Kratochwil, E. M. Carreira and K. Müller, *J. Fluorine Chem.*, 2017, **198**, 34–46.

23 (*a*) G. R. Ott, K. Gibson, B. Lefker, P. Humphries, Orexin-2 receptor agonists, *WO Pat.*, 167925, 2023; (*b*) A. Dumoulin, P. M. Blom, A. Daugan, M. Laugeois, C. G. Housseman, A. Denis, Y. Lamotte, A. Le Tiran, K. Christensen, Leucine-Rich Repeat Kinase 2 inhbitors, *WO Pat.*, 194976, 2022.

24 Q. A. Huchet, B. Kuhn, B. Wagner, N. A. Kratochwil, H. Fischer, M. Kansey, D. Zimmerli, E. M. Carreira and K. Müller, *J. Med. Chem.*, 2015, **58**(22), 9041–9060.
25 S. J. Stachel, C. A. Coburn, S. Sankaranarayanan, E. A. Price, B. L. Pietrak, Q. Huang, J. Lineberger, A. S. Espeseth, L. Jin, J. Ellis, M. K. Holloway, S. Munshi, T. Allison, D. Hazuda, A. J. Simon, S. L. Graham and J. P. Vacca, *J. Med. Chem.*, 2006, **49**(21), 6147–6150.
26 T. J. Cogswell, A. Dahlén and L. Knerr, *Chem.–Eur. J.*, 2019, **25**, 1184–1187.
27 T. Fujita, K. Sugiyama, S. Sanada, T. Ichitsuka and J. Ichikawa, *Org. Lett.*, 2016, **18**(2), 248–251.
28 *Mnova – Mspin*.
29 A. Y. S. Balazs, R. J. Carbajo, N. L. Davies, Y. Dong, A. W. Hird, J. W. Johannes, M. L. Lamb, W. McCoull, P. Raubo, G. R. Robb, M. J. Packer and E. Chiarparin, *J. Med. Chem.*, 2019, **62**, 9418–9437.
30 G. H. Goetz, W. Farrell, M. Shalaeva, S. Sciabola, D. Anderson, J. Yan, L. Philippe and M. J. Shapiro, *J. Med. Chem.*, 2014, **57**, 2920–2929.
31 (*a*) P. Shah and A. D. Westwell, *J. Enzym. Inhib. Med. Chem.*, 2007, **22**(5), 527–540; (*b*) S. Purser, P. R. Moore, S. Swallow and V. Gouverneur, *Chem. Soc. Rev.*, 2008, **37**, 320–330.
32 (*a*) R. S. Obach, G. S. Walker and M. A. Brodney, *Drug Metab. Dispos.*, 2016, **44**, 634–646; (*b*) Y. Pan, *ACS Med. Chem. Lett.*, 2019, **10**, 1016–1019; (*c*) B. M. Johnson, Y.-Z. Shu, X. Zhuo and N. A. Meanwell, *J. Med. Chem.*, 2020, **63**(12), 6315–6386.